

MATERIAL TESTING OF MICRO-CONCRETE AND 3D-PRINTED REINFORCEMENT FOR USE IN SMALL-SCALE SEISMIC TESTING OF RC STRUCTURES

Medhat Elmorsy^{1,2*}, Rafal Wrobel³, Christian Leinenbach³, Michalis F. Vassiliou¹

¹Chair of Seismic Design and Analysis, Institute of Structural Engineering (IBK),
ETH Zürich Stefano-Franscini-Platz 5 8093 Zürich, Switzerland
{medhat.elmorsy, vassiliou}@ibk.baug.ethz.ch

²Structural Engineering Department, Mansoura University, Mansoura, Egypt

³EMPA, Swiss Federal Laboratories for Materials Science and
Technology Überlandstrasse 129, CH-8600 Dübendorf
{rafal.wrobel, christian.leinenbach}@empa.ch

Abstract

A framework for small scale modeling of RC structures that helps understanding their seismic behavior is discussed in this paper. The framework includes testing of small scale RC buildings manufactured using micro concrete and additively manufactured (3D printed) reinforcement cages on a shake table mounted on a geotechnical centrifuge. This paper presents material level testing of micro-concrete and 3D printed reinforcement that are to be used in the proposed framework. Mechanical properties of the 3D printed rebars are first discussed and compared to full scale rebar mechanical properties. A Concept Laser M2 Laser Powder Bed Fusion (LPBF) printer is used for printing the rebars. In addition, the compressive and tensile behavior of micro-concrete are studied using small scale cylinders and beams (for four-point bending tests), respectively. The results of this paper reveal that the mechanical properties of 3D printed submillimeter rebars can be adjusted by modulating the printing parameters. Moreover, concrete mechanical properties that are suitable for the discussed framework can be achieved.

Keywords: 3D printed reinforcement, Global level assumptions, Small scale modeling, Reinforced concrete structures.

1 INTRODUCTION: THE NEED FOR SMALL SCALE TESTING

Experimental testing has always played a vital role in pushing the limits imposed on structural design by modelling uncertainties. Moncarz and Krawinkler [1] identified three basic objectives for which experimental testing is generally conducted; (1) develop or verify component-level force deformation relationships (2) establish loading criteria for environmental effects such as wind and earthquakes (3) study of the structure-level behavior. Structure-level tests are necessary for the validation of the global level (system level) assumptions. Examples of global level assumptions are the ones related to boundary conditions, interaction of components, damping model, numerical integration scheme. In an opinion paper by Bradley [2], these global level assumptions have been identified as a major source of error in numerical modeling of earthquake engineering problems. Uncertainty in earthquake engineering can be categorized into two main classes; ground motion uncertainty (e.g., [3], among others) and modeling uncertainty (e.g., [4-6], among others). Currently, time history analysis is considered as the state of the art in modeling the seismic response of RC structures at the system level. Its most widespread validation procedure is the test of predicting the response of a RC structure tested on a shaking table. However, blind prediction contests show that the contestants fail in predicting the response of the tested specimens with reasonable accuracy, even for structures much simpler than the ones constructed in practice, and even when the structural properties and the measured excitation are given to the contestants [7].

For instance, the simple RC column shown in Figure 1 (left) was tested on the shaking table of UCSD in 2010 under 6 ground motions [8, 9]. A total of 41 expert teams were invited to predict the response. The measured response and the predictions for the maximum top displacement are indicatively shown in Figure 1 (middle). There is a large dispersion in the numerical results and many predictions grossly underestimate or overestimate displacements. Interestingly, after the test series of the six earthquakes, the column did not appear to have failed. However, only 14 out of 41 contestants predicted non-failure, while the rest predicted failure. Within the group that predicted failure, there was a large dispersion related to the mode of failure (Figure 1, right). Similar observations were also seen in the blind prediction contest for a shear wall building slice tested by Panagiotou et al. [10].

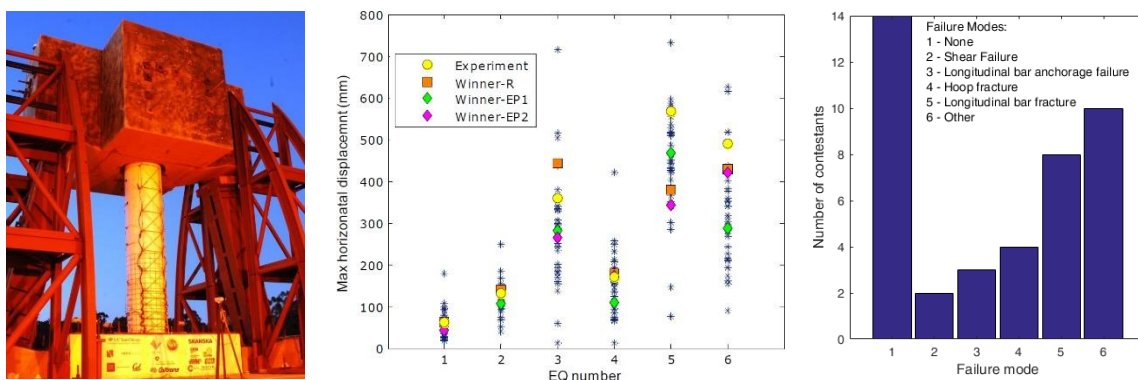


Figure 1: Left: Bridge column tested in UCSD [9]. Middle: Maximum top displacements predicted by the blind prediction contest contestants [8]. Right: Number of predictions for each of the six suggested failure modes [4].

This lack of match between mathematical modeling and experiments happened despite the fact that in such contests, the material level uncertainty is reduced by providing to the contestants the material properties. Moreover, blind prediction contests for cyclic component-

level tests show much better results than the system-level ones [11, 12]. These observations emphasize the importance of validation of the global level assumption.

In parallel, conventional validation test of numerically reproducing the experimentally obtained response to a particular ground motion with acceptable accuracy is too strict of a validation test for structural models [13, 14]. The Earthquake Engineering design problem involves predicting the statistics of the response to an ensemble of ground motions characterizing a given seismic hazard; not to a single ground motion. This is a weaker model validation test that requires that the structural model only be unbiased and introduce less uncertainty than the uncertainty introduced by the excitation itself. In other words, models that can be designated “good”, in the scope of earthquake engineering, should introduce less uncertainty than the already-existing motion-to-motion variability [15, 16]. Such statistical procedure is possible at a material or component level, but it is currently impossible at a system level due to the prohibitive cost of performing multiple shake table tests with virgin identical specimens. Moreover, this lack of adequate data has led to very different approaches in modelling, without the experimental tools to create enough data to statistically accept or reject the hypotheses behind them. It is this lack of experimental tools that has led to disagreements between major figures of structural earthquake engineering, in terms of modelling approaches. We believe that this lack of consensus in modelling approaches and the degree of structural modelling accuracy constitutes a major research gap. Therefore, there is a need to develop a methodology to perform low cost system-level seismic testing of RC structures, so that it can be performed multiple times and increase the datasets that we have to calibrate our models on.

To this end, this paper illustrates a framework for small scale (on the order of 1:30 – 1:40) testing of RC structures. The framework is explained in detail in the next section. After illustrating the proposed framework, this paper offers a brief summary of the efforts done as a feasibility study of this framework. Consequently, this paper presents material level testing of micro-concrete and 3D printed reinforcement that are to be used in the proposed framework. Mechanical properties of the 3D printed rebars are first discussed and compared to full scale rebar mechanical properties. In addition, the compressive and tensile behavior of micro-concrete are studied via testing small scale cylinders and beams (for four-point bending tests), respectively.

2 PROPOSED FRAMEWORK

This section outlines the framework to validate the global level assumptions that was outlined in the previous section. The framework has two main goals: (1) to develop a methodology for physical modelling of RC at a very small scale. The methodology will be based on 3D printing. We focus on modern (i.e. of the last 30-40 years) ductile buildings to avoid issues related to scaling of shear strength and of bonding behavior (2) to use this approach to statistically evaluate some major assumptions that the structural engineering research community makes to scale up from component-level cyclic behavior to system-level dynamic behavior.

To this end, scaled models (on the order of 1:30) will be constructed and tested both statically and dynamically using a shake table mounted on a geotechnical centrifuge. The scaled reinforcement will be 3D printed using a metal 3D printer, to make the construction of multiple specimens timewise feasible – something that was not possible before 3D printing. Material and component level tests will be performed at the model scale, so that values directly obtained at the scale of the shake table tests are used as input in the numerical models. Although efforts are made to avoid model distortions, it should be acknowledged that scaled models may have some degree of distortion, as concrete properties scale with size, even when scaled aggregates

are used. However, our specimens will serve for numerical model validation of the global level assumptions for given (tested) material and component properties.

3 FEASIBILITY STUDY

Recently, as a feasibility study, compression tests of micro-concrete (gypsum and fine silica sand) cylindrical specimens and bending tests of micro-RC beams were performed [17] (Figure 3a). The concrete had a compression strength ranging from 15 to 25 MPa (obtained from tests on 50 x 112 mm cylinders, depending on the mixture ratio and on the type of gypsum) and a tension strength of 2 to 8 MPa obtained from 4-point bending tests on 10 x 10 x 80 mm plain concrete beams). In addition, 3D printed reinforcement was provided for 12.5 x 12.5 x 70 mm beams using Laser Powder Bed Fusion (LPBF) printing technology. The stirrups had a diameter of 0.35 mm and the longitudinal reinforcement a diameter of 0.6 mm (1:40 scaled models of $\Phi 14$ and $\Phi 24$). The yield strength of the reinforcement was around 400 MPa. The force-deformation curve of the small-scale reinforced concrete beam agreed well with preliminary numerical results obtained with Opensees software platform (using Mander et al. [18] concrete material model).

In addition, Del Giudice et al. [19] performed cyclic tests on 5 small scale micro-concrete beams reinforced with 3D printed stainless steel reinforcement cages (Figure 3b). Concrete with cement/sand/water ratio of 1/1/0.5 by weight was used. All the tested beams failed in bending mode in which fracture of the longitudinal reinforcement was observed. According to their test campaign, the construction of small-scale models was feasible and the behavior of the tested beams resembled the full-scale behavior in terms of strengths and stiffness. Moreover, their numerical models (using Opensees) captured most of the cyclic behavior of the concrete beams. However, there were some limitations: (a) the setup could not apply axial load on the specimens, so only beams (not columns) could be tested (b) there was high variability in steel mechanical properties (c) the numerical analysis performed could not capture the post-peak degradation behavior (d) no characterization of bond behavior between micro-concrete and 3D printed steel was performed. These limitations are to be addressed in this paper.

4 3D PRINTED STEEL TENSILE TESTING

In order to study the mechanical properties of the 3D reinforcing bars, two batches of steel rebars were manufactured by Laser Powder Bed Fusion (LPBF) using a Concept Laser M2 printer that is able to manufacture various types of metal. A gas-atomized stainless steel 316L powder with a mean powder diameter of $\sim 32 \mu\text{m}$ was used as a feedstock material. The printing parameters of each batch are shown in Table 1. Two rebar diameters were tested; 0.8 mm and 0.4 mm, corresponding to 24 mm and 12 mm reinforcing bars in the prototype scale, if a 1:30 scale is assumed. Six rebars were tested for each diameter to evaluate the dispersion among similar rebars. Two different rib configurations were tested; plain rebars (P) and ribbed rebars (D1) with rib parameters as shown in Table 2 according to EN:10080 standard [20]. The rebar with 0.4 mm diameter was only tested with plain surface (without ribs) for two reasons: a) when printing the rebar with ribs, the ribs were barely printed due to the lower accuracy of the printer for such small details b) the 0.4 mm rebar was intended to be used as shear reinforcement (stirrups) in the proposed framework where ribs are not significant. An optical microscope was used to measure the actual diameter of the rebars and to check the general surface deformation of the rebars.

A 200 kN Universal Testing Machine (UTM) at the ETH Zurich was used to perform the tensile tests. Figure 3 shows the test setup used to perform the tests. A pair of 1 kN tension grips were attached to the machine. The specimens were tested under monotonically increasing

displacement with strain rate of 0.015 (1.5%) mm/mm/minute according to [21] until fracture occurs. The strain rate was controlled by the movement of the cross head of the UTM. Strain was also measured using an extensometer attached to the rebar. A 10 kN load cell was used to measure the applied load.

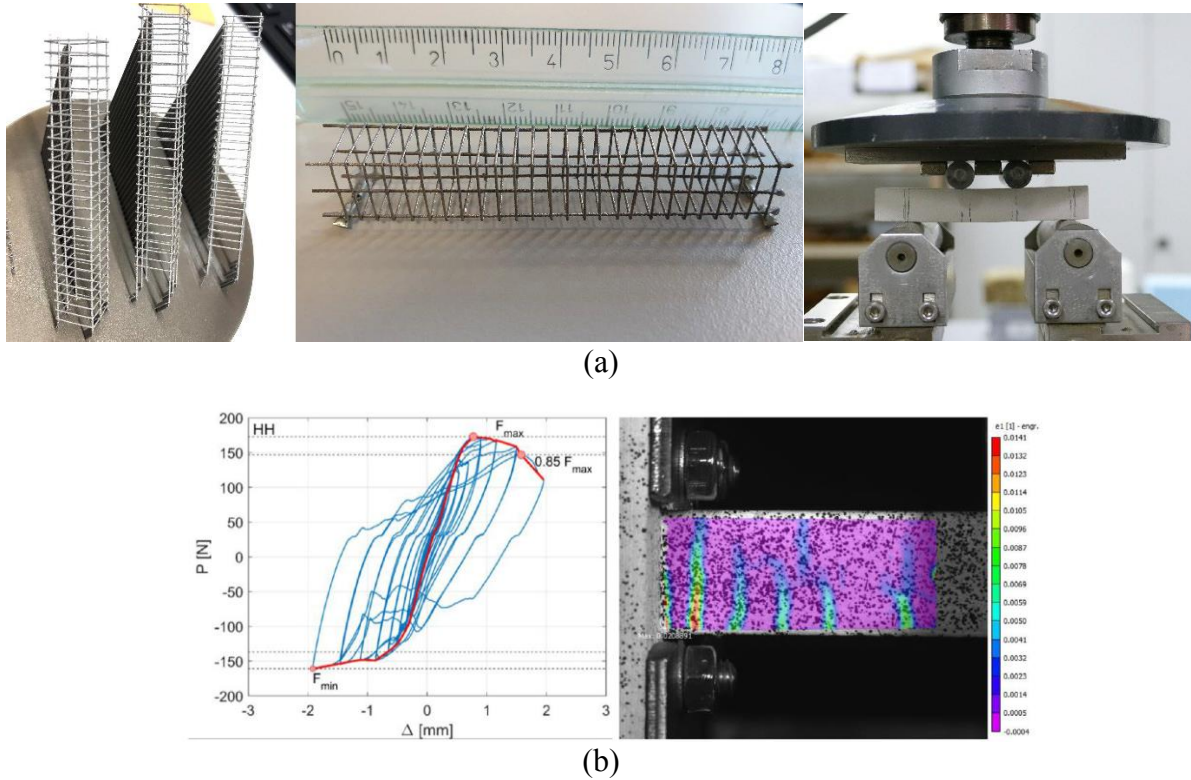


Figure 2: (a) Four-point bending tests on 3D printed steel reinforced micro-concrete beams [17] (b) Lateral cyclic loading tests on 3D printed steel reinforced micro-concrete columns [19].

Batch	Laser power [W]	Scanning speed [mm/s]	Hatch spacing [mm]	Layer thickness [mm]	Printing orientation [°]	Number of contours	Contour distance [mm]
I	110	300	0.01	0.03	45	1	0.075
II	110	300	0.01	0.03	45	2	0.06

Table 1: Printing characteristics of the tensile test specimen batches.

Category	h	c	β
EN:10080 [20] recommended range	0.03d:0.15d*	0.40d:1.20d	35°:75°
D1	0.10d	1.00d	63.43°

*d is the rebar diameter.

Table 2: Transverse rib parameters for the tested rib configuration.

5 CONCRETE COMPRESSION AND FOUR-POINT BENDING TESTS

Two concrete mixes were used to identify favorable concrete mechanical properties that are comparable to prototype scale properties. Two binders were tried according to Table 3. The water binder ratio (W/B) was 0.5 and 0.7 for the mix with cement (mix A) and gypsum (mix B)

binder, respectively. For the two mixes, the sand binder (S/B) ratio was kept constant at 1.0 based on studies by [19, 22]. The sand used in all mixes was Perth silica sand (Crystalline silica SiO_2). The testing of the cement concrete mix had been previously tested by Del Giudice et al. [19]. However, since the cement concrete compressive strength, tensile strength, and bond behavior was not comparable to that of the prototype ones as discussed later in this paper, the gypsum mix was manufactured and tested.

Cylinders of 15 mm diameter and 30 mm height were tested under uniaxial compression. For the four-point bending test, beams with 15 mm x 15 mm cross section and 80 mm length (shear span was equal to 20 mm). For each mix, six cylinders and six beams were tested to evaluate the dispersion of flexural and compression strength. A PLA (Polylactic acid) 3D printer was used to print the beam molds while for the cylinder molds, PVC pipes with 15 mm inner diameter were used as molds and then the specimens were cut into 30 mm high pieces.

The same 200 kN UTM with the appropriate attachments was used to perform the compression and the four-point bending on concrete samples. The loading was applied with displacement-controlled increments corresponding to a strain rate of 1×10^{-5} mm/mm/second until failure. Such a strain rate was chosen according to [18] so that strain rate does not affect the behavior of the tested samples.

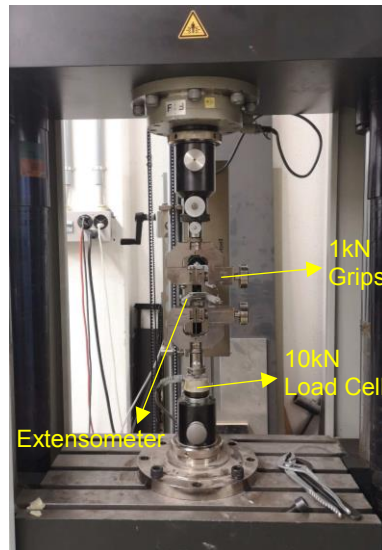


Figure 3: Test Setup for the performed tensile tests.

Mix	Binder	Binder Commercial name	S/B	W/B	Additives
A	Cement	Holcim CEM I 42.5N (Normo 4)	1.0	0.5	1.0g of Master MasterGlenumACE30 (Superplasticizer)
B	Gypsum	Prestia Tradition Plaster	1.0	0.7	-

Table 3: Concrete mix details

6 TEST RESULTS

6.1 Tensile test of reinforcing bars

The stress strain relationship of the 3D printed steel is shown in Figures 4 and 5 for batches I and II, respectively. The average (AVG) and the variability of the data measured by the

coefficient of variation (COV) of the main features of the stress strain relationships is summarized in Table 4. These main features are: a) Elastic modulus (E_s) b) Yield strength (f_y) c) Ultimate strength (f_u) d) Ratio of ultimate to yield strength (T/Y) e) Ratio of post yield modulus to elastic modulus (α) f) Maximum strain (ϵ_{su}). Yield Strength value was calculated using the offset of 3‰ as suggested by ASTM E8/E8M-21. In addition, the characteristic parameter values according to the Eurocode for design of concrete structures EC2 [23] are shown in Table 4. These values correspond to 5%, 10%, and 10% percentiles for f_y , T/Y , and ϵ_{su} parameters and are reported to evaluate the resemblance of the small-scale 3D printed rebars to their prototype scale counterparts and the related design code requirements.

According to the Eurocode (EC2), reinforcing bars are divided into three classes according to ductility; A, B, and C with A being the least ductile and C being the most ductile. The requirements for ductility of reinforcing bars in EC2 are as follows:

1. Characteristic yield strength should be in the range of 400 – 500 MPa for all the three ductility classes. The upper limit of the code is imposed for ensuring enough ductility since high yield strength can significantly reduce ductility. The deformed rebars (D1) in the two batches satisfied this requirement. However, the larger diameter plain rebars had yield strength which is lower than the lower limit of the code range of 400 MPa (97.5% and 88.9% of the code minimum for batches I and II, respectively).
2. The ratio of characteristic ultimate strength to the characteristic yield strength (T/Y ratio) should be at least 1.05, 1.08, 1.15 for ductility classes A, B, and C, respectively. The T/Y ratio is mainly responsible for the distribution of plastic deformation over larger distance and avoiding local strain concentrations [24]. Larger T/Y ratios can increase member ductility by increasing the distance over which plastic deformations are distributed [24, 25]. For batch I, all the tested 3D printed bar batches had T/Y ratios of more than 1.21, satisfying the requirements of ductility class C indicating good ductility properties of the rebars from the T/Y point of view. For batch II, only the 0.4 mm bar satisfied class C requirements – while the other rebars satisfied class B requirements.
3. The characteristic ultimate elongation (strain), ϵ_{suk} , should be at least 2.5%, 5%, and 7.5% for ductility classes A, B, and C, respectively. Along with lower yield strength and high T/Y ratio, increasing the ultimate strain capacity can significantly affect reinforced concrete member ductility. Hassan and Elmorsy [24], based on parametric section analysis, showed that increasing the ultimate steel strain capacity increases the section ductility by up to 100%. Increasing the ultimate steel strain capacity from 0.05 to 0.10 yielded about 100% increase in section curvature ductility [24]. For batch I, the tested rebars had high strain capacities ranging from 6.33% (0.4 mm plain rebar) to 14.06% (0.8 mm plain rebar) indicating high ductility and satisfying ductility class B (for the 0.4 mm plain rebar) and ductility class C (for other rebars) requirements. On the other hand, for batches II, the deformed bars had higher strain capacities (3.28%) than plain rebars. The 0.8 mm deformed rebars in batches II lied between the requirements of the ductility classes A and B. Taking into consideration that the 0.4 mm plain rebars are intended to model stirrups in the proposed framework, the ductility of these rebars are typically not important, especially for modern structures that are mainly designed to fail in flexural hinging mode. The 0.8 mm plain rebars had low maximum strain capacity - ϵ_{suk} was 2.32 for batches II, which is below the limit of the least ductile reinforcing bars class of ductility (class A).

On a different note, the variability of the yield strength, ultimate strength, and, accordingly, the T/Y ratio was small (the COV was 6.1% as a maximum value among the three parameters). On the other hand, the variability of the elastic modulus and maximum strain was generally higher. This high variability of the maximum strain capacity contributed to the low characteristics maximum strain compared to the mean/median values.

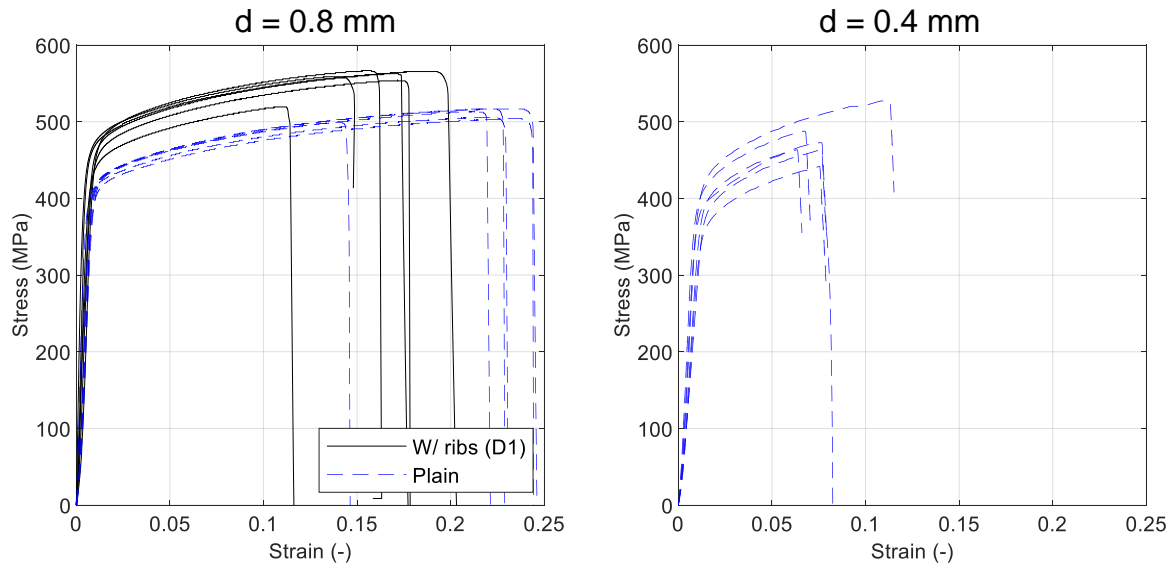


Figure 4: Stress strain relationships of rebar from Batch I.

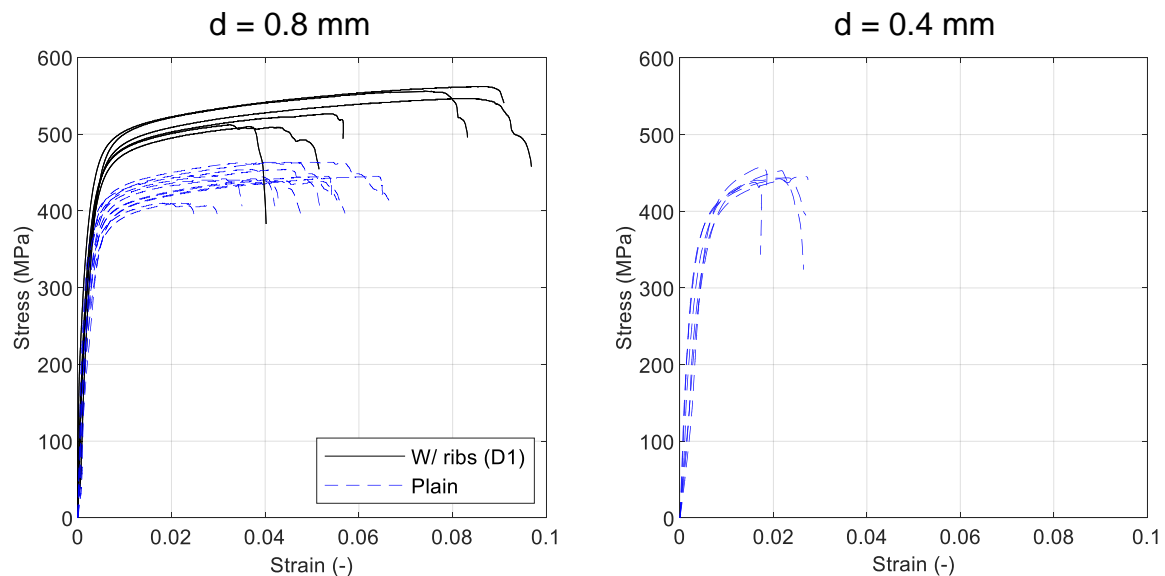


Figure 5: Stress strain relationships of rebar from Batch II.

6.2 Concrete compression and four-point bending tests

This section discusses the compressive (f_c) and tensile strength (represented by the modulus of rupture, f_r) of the two mixes tried in this paper. The cement concrete was left to cure for 28 days before testing while the gypsum concrete was left for only 14 days. The cement concrete mix had average compressive strength 41.04 MPa and the modulus of rupture was 10.38 MPa. The measured modulus of rupture is 250% larger than what ACI 318-19 code [26] predicts ($f_r = 0.62\sqrt{f_c} = 3.97$ MPa). While the compressive strength is typical and is frequently encountered in full scale structures, the tensile strength is much higher than the prototype strength which is intelligible because of size effects [27]. The tensile strength of concrete is an important parameter affecting the concrete strength in diagonal tension and resistance to shear, bond strength with bars, and cracking load levels and crack patterns [27]. Therefore, the proper scaling of tensile strength is vital for replication of failure modes and cracking pattern. This

observation motivated the use of other gypsum as a binder instead of cement since it was observed to be less prone to scale effects in previous studies [22, 27, 28].

Batch	Nominal Diameter [mm]	Actual Diameter [mm]	Rib configuration		E_s [MPa]	f_y (Y) [MPa]	f_{yk} [MPa]	f_u (T) [MPa]	T/Y	$(T/Y)_k$	α [%]	ε_{su} [%]	ε_{suk} [%]
I	0.80	0.75	P	AVG	71375	396.9	390.2	509.3	1.28	1.26	0.71	20.0	14.06
				COV	0.203	0.011	-	0.014	0.014	-	0.193	0.167	-
	0.80	0.75	D1	AVG	82848	440.3	411.6	554.5	1.26	1.21	0.68	15.0	10.8
				COV	0.270	0.048	-	0.032	0.048	-	0.281	0.178	-
	0.40	0.33	P	AVG	40226	381.9	344.8	476.0	1.25	1.21	2.91	7.8	6.33
				COV	0.183	0.052	-	0.061	0.033	-	0.179	0.212	-
II	0.80	0.96	P	AVG	198725	371.7	355.6	442.3	1.19	1.14	0.57	4.2%	2.32
				COV	0.101	0.053	-	0.041	0.043	-	0.142	0.313	-
	0.80	0.96	D1	AVG	193637	452.4	450.9	535.4	1.18	1.12	0.54	6.0	3.28
				COV	0.056	0.032	-	0.042	0.026	-	0.095	0.357	-
	0.40	0.56	P	AVG	174340	363.3	339.0	450.9	1.25	1.16	1.88	2.1	1.62
				COV	0.310	0.068	-	0.017	0.069	-	0.459	0.177	-

Table 4: Tensile test results summary.

For mix B, the average compressive strength was much lower reaching 19.93 MPa. Moreover, the COV for the compressive strength and modulus of rupture were 0.08 and 0.04, respectively. Comparing to prototype scale, the modulus of rupture of mix B was 4.14, which makes it only 49% larger than what ACI 318-19 code [26] predicts ($f_r = 0.62\sqrt{f_c} = 2.77$ MPa) – indicating an improvement compared to mix A.

Mix	Binder	S/B	W/B	f_c (AVG) [MPa]	f_c (COV)	f_r (AVG) [MPa]	f_r (COV)	f_r/f_c (AVG)
A	Cement	1.0	0.5	41.04	0.11	10.38	0.14	0.25
G	Gypsum	1.0	0.7	19.93	0.08	4.14	0.04	0.21

Table 5: Results of compression and four-point bending tests.

7 CONCLUSIONS

This paper illustrated a framework for small scale (on the order of 1:30 – 1:40) testing of RC structures. Moreover, this paper presents material level testing of micro-concrete and 3D printed reinforcement that are to be used in the proposed framework. Mechanical properties of the 3D printed rebars are first discussed and compared to full scale rebar mechanical properties. In addition, the compressive and tensile behavior of micro-concrete are studied via testing small scale cylinders and beams (for four-point bending tests), respectively. Through the test results of the material tests performed in this paper, the following conclusions can be drawn:

- The mechanical properties of 3D printed submillimeter rebars can be adjusted by modulating the printing parameters. Moreover, concrete mechanical properties that are suitable for the discussed framework can be achieved.
- Obtaining mechanical properties of 3D printed submillimeter bars that are comparable to full scale prototype rebars seems feasible.
- Attention should be paid to scaling effects of concrete in tension and bonding since these both properties control cracking pattern and failure mode. Using gypsum as a binder produced closer concrete mechanical properties as compared to full scale concrete.

ACKNOWLEDGEMENTS

This work was supported by the ETH Zurich under grant ETH-11 21-1.

REFERENCES

- [1] P. Moncarz, H. Krawinkler. Theory and Application of Experimental Model Analysis in. Earthquake Engineering, John A Blume Earthquake Engineering Center, Department of Civil Engineering, Stanford, Calif. 1981.
- [2] B.A. Bradley. A critical examination of seismic response uncertainty analysis in earthquake engineering. *Earthquake engineering & structural dynamics*. 2013;42(11):1717-29.
- [3] M. Elmorsy, M.F. Vassiliou. Effect of ground motion processing and filtering on the response of rocking structures. *Earthquake Engineering & Structural Dynamics*. 2023.
- [4] M. Elmorsy. Nonlinear Modeling Parameters for Beam-Column Joints in Seismic Analysis of Concrete Buildings: Master Thesis, University of Alaska Anchorage; 2020.
- [5] W.M. Hassan, M. Elmorsy. Probabilistic Beam-Column Joint Model for Seismic Analysis of Concrete Frames. *Journal of Structural Engineering*. 2022;148(4):04022011.
- [6] W.M. Hassan WM, M. Elmorsy. Cyclic nonlinear modeling parameters for unconfined beam-column joints. *ACI Struct J*. 2022;119(1):89-104.
- [7] P. Fajfar. Analysis in seismic provisions for buildings: past, present and future. Recent Advances in Earthquake Engineering in Europe: *16th European Conference on Earthquake Engineering*-Thessaloniki 2018; 2018: Springer.
- [8] V. Terzic, M.J. Schoettler, J.I. Restrepo, S.A. Mahin. Concrete column blind prediction contest 2010: outcomes and observations. *PEER Report*. 2015;1(2015):1-145.
- [9] M.J. Schoettler, J.I. Restrepo, G. Guerrini, D.E. Duck, F. Carrea. A full-scale, single-column bridge bent tested by shake-table excitation. Center for Civil Engineering Earthquake Research, Department of Civil Engineering, University of Nevada. 2012.
- [10] M. Panagiotou, J.I. Restrepo, J.P. Conte. Shake-table test of a full-scale 7-story building slice. Phase I: Rectangular wall. *Journal of Structural Engineering*. 2011;137(6):691-704.
- [11] M. Trüb. Numerical modeling of high-performance fiber reinforced cementitious composites. *IBK Bericht*. 2011;333.
- [12] X. Lin, X. Lu. Numerical models to predict the collapse behavior of RC columns and frames. *The Open Civil Engineering Journal*. 2017;11(1).
- [13] J. Bachmann, M. Strand M, M.F. Vassiliou, M. Broccardo, B. Stojadinovic. Is rocking motion predictable? *Earthquake Engineering & Structural Dynamics*. 2018;47(2):535-52.
- [14] J. Bachmann, M. Strand M, M.F. Vassiliou, M. Broccardo, B. Stojadinovic. Modelling of rocking structures: Are our models good enough? *Online Proceedings: 2nd International Conference on Natural Hazards & Infrastructure (ICONHIC 2019)*; 2019: National Technical University of Athens.

- [15] A.A. Katsamakas, M.F. Vassiliou. Finite element modeling of free - standing cylindrical columns under seismic excitation. *Earthquake Engineering & Structural Dynamics*. 2022;51(9):2016-35.
- [16] A.A. Katsamakas, M.F. Vassiliou. Experimental parametric study and phenomenological modeling of a deformable rolling seismic isolator. *Earthquake Engineering and Structural Dynamics* (accepted for publication). 2022.
- [17] L. Del Giudice, R. Wróbel, C. Leinenbach, M.F. Vassiliou. Static testing of additively manufactured microreinforced concrete specimens for statistical structural model validation at a small scale. *8AESE Abstract Book*. 2020:78-85.
- [18] J.B. Mander, M.J. Priestley, R. Park. Theoretical stress-strain model for confined concrete. *Journal of structural engineering*. 1988;114(8):1804-26.
- [19] L. Del Giudice, R. Wróbel, A.A. Katsamakas, C. Leinenbach, M.F. Vassiliou. Physical modelling of reinforced concrete at a 1: 40 scale using additively manufactured reinforcement cages. *Earthquake Engineering & Structural Dynamics*. 2022;51(3):537-51.
- [20] EN:10080, Steel for reinforcement of concrete – weldable reinforcing steel – general. 2021.
- [21] Standard test methods for tension testing of metallic materials: ASTM international; 2016.
- [22] J. Knappett, C. Reid, S. Kinmond, K. O'Reilly. Small-scale modeling of reinforced concrete structural elements for use in a geotechnical centrifuge. *Journal of Structural Engineering*. 2011;137(11):1263-71.
- [23] Eurocode 2: Design of concrete structures—. Part. 2004;1(1):230.
- [24] W.M. Hassan W, M. Elmorsy. Database trends and critical review of seismic performance tests on high strength steel reinforced concrete components. *Engineering Structures*. 2021; 239:112092.
- [25] D. Sokoli. Fracture of high-strength bars in concrete frame members under earthquake loads: PhD Thesis, The University of Texas at Austin; 2018.
- [26] H.G. Harris, G. Sabnis. Structural modeling and experimental techniques: CRC press; 1999.
- [27] M. Loli, J.A. Knappett, M.J. Brown, I. Anastasopoulos, G. Gazetas. Centrifuge modeling of rocking - isolated inelastic RC bridge piers. *Earthquake engineering & structural dynamics*. 2014;43(15):2341-59.
- [28] Building code requirements for structural concrete (ACI 318-19) and commentary, 2019: American Concrete Institute.